Proceedings of the Second International Conference on Press-in Engineering 2021, Kochi, Japan – Matsumoto et al (eds)
© 2021 Taylor & Francis Group, London, ISBN 978-1-032-10414-0

Results of static vertical load tests on tubular piles installed by Standard Press-in and Rotary Cutting Press-in

K. Okada, K. Inomata & Y. Ishihara
GIKEN LTD., Kochi, Japan

ABSTRACT: The Press-in Method, being started with Standard Press-in (SP, press-in without installation assistance), has expanded its applicability to hard ground conditions with the development of Press-in with Augering and Rotary Cutting Press-in (RCP, press-in with the use of rotational forces onto a pile with cutting teeth on its base). Although the piles installed by these methods are usually used for retaining walls, there have recently been an increasing number of cases where SP piles and RCP piles are used for foundations. To understand the performance of these piles and establish rational design methods, it is necessary to accumulate load test results with different pile specifications and in different ground conditions. This paper reports the records of installation and the results of static vertical load tests on two piles with the outer diameter of 1000mm and the thickness of 12mm, which were installed by SP or RCP in the same site.

1 INTRODUCTION

Among several installation techniques in the Press-in Method (IPA, 2016), Standard Press-in (SP) installs a pile without any installation assistance such as water jetting and augering, and it is suitable for soft ground conditions. The applicability of the Press-in Method to hard grounds has been significantly improved by the development of penetration techniques such as Press-in with Augering and Rotary Cutting Press-in Method (RCP, with the use of vertical and rotational forces onto a pile with cutting teeth on its base). Although piles installed by these installation techniques are usually used for retaining walls, there have recently been some cases where RCP piles are used for foundations. On the other hand, SP piles are beginning to be used as non-temporary structures (e.g. Tanaka *et al.*, 2018), in which they are supposed to resist to vertical loads. To understand the performance of these piles and establish a rational design method, it is necessary to accumulate load test results with different pile specifications and in different ground conditions.

This paper reports the records of installation and the results of static vertical load tests on two piles with the outer diameter of 1000mm and the thickness of 12mm, which were installed by Standard Press-in or Rotary Cutting Press-in.

2 METHOD OF FIELD TESTS

2.1 *Site profile and test piles*

Figure 1 shows the results of SPT in the test site. The ground consists of soft alluvial soils. For the depth (z) from 0m to 4m, the ground contains gravels, which is reflected in relatively high SPT N values. In 4m < z < 23m, it consists of soft sand and silt with SPT N being smaller than 10, except for a relatively large value of 19 at around z = 8m. Below 23m is a hard sand and gravel layer with SPT N exceeding 50.

Two piles (A and B) with the outer diameter of 1000mm and the thickness of 12mm were used as test piles in the field tests. The specification of the test piles is shown in Table 1. Pile A had its embedment depth of 24m and was installed by Rotary Cutting Press-in into the sand and gravel layer with SPT N value exceeding 50. It was instrumented with strain gauges at several sections for measuring axial strains, as shown in Figure 1. Pile B had its embedment depth of 8m and was installed by Standard Press-in into a silty sand layer with SPT N being around 19.

2.2 *Test layout and procedures*

The test layout is shown in Figure 2. Pile A was positioned in between the two sheet pile walls with the embedment depth of 14.4m, which were used as reaction piles during static vertical load test. Pile B was

DOI: 10.1201/9781003215226-7

Table 1. Specification of test piles.

		Pile A	Pile B
Installation method		RCP	SP
Outer diameter (D_o)	mm	1000	1000
Pile thickness	mm	12	12
Pile length	m	25	9
Final installation depth	m	24	8
Number of teeth		6	6

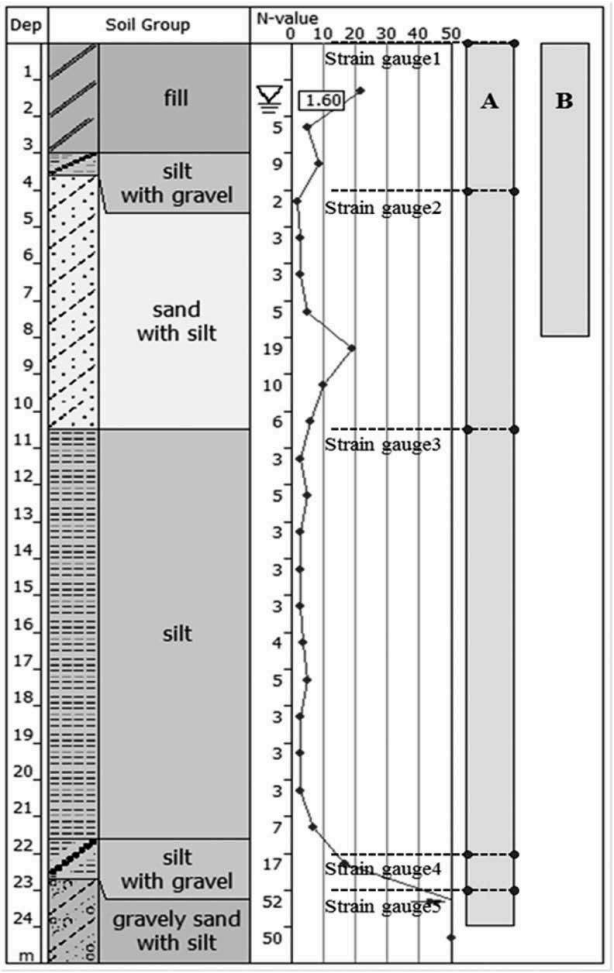

Figure 1. Site profile and test piles.

positioned slightly away from the sheet pile walls compared with pile A. The distance between the test piles and the sheet pile walls were greater than $3D_o$ (where D_o is the pile outer diameter) to avoid the influence of the walls on the pile capacity (JGS, 2002).

The field test was conducted with the following procedures.

Firstly, Pile A was installed by Rotary Cutting Press-in using a press-in machine (F401) while gaining a reaction force from a self-weight system as shown in Figure 3. The installation was associated with load-controlled surging, in which the pile was extracted when the jacking force applied by the press-in machine (Q') or the torque applied by the

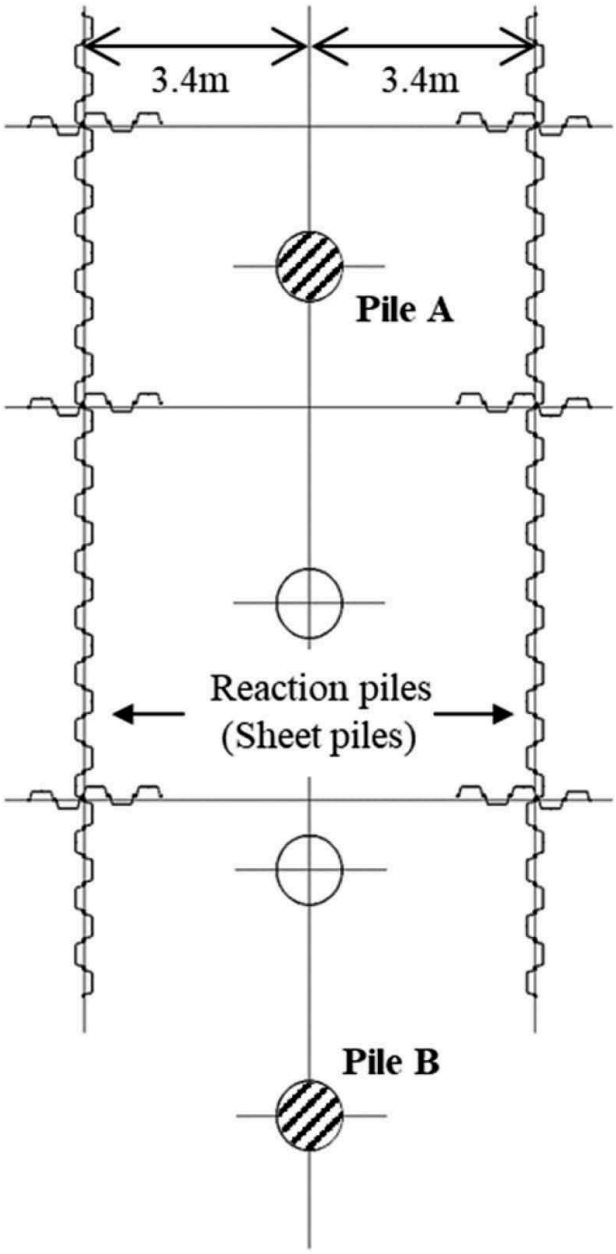

Figure 2. Test layout.

press-in machine (T') reached their upper-bound values (Q'_{UL} or T'_{UL}). Water was injected in the pile base, with the flowrate (f_w) being maintained at 15 liters per minute in 0m < z < 23m and being minimized in deeper than 23m. At the end of installation, termination load (Q_T) was applied for a certain period of time, without rotation and water injection.

Secondly, Pile B was installed by Standard Press-in using a press-in machine (F401) while gaining a reaction force from the same self-weight system as was used for Pile A. The installation was associated with load-controlled surging except for the last 1m, where it was conducted monotonically (without extraction). Water injection was not used. At the end of installation, termination load (Q'_T) was applied for a certain period of time without water injection. The jacking force and the penetration depth were measured by an automatic measurement system equipped in the press-in machine.

Figure 3. Press-in machine with Self-weight system.

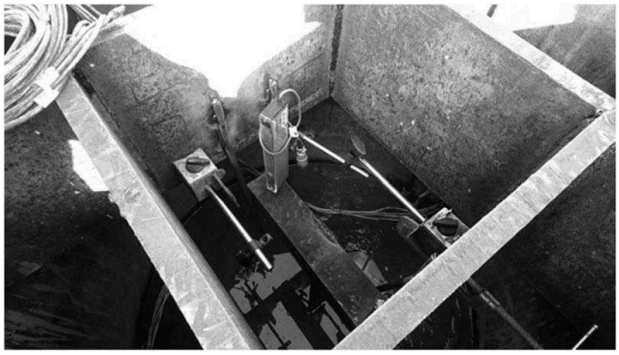

Figure 4. Displacement measurement for inner soil column.

Thirdly, the sheet piles were installed by Standard Press-in using a press-in machine (F111).

Finally, static vertical load tests were conducted on Piles B and A when 25 days and 57 days had passed since the end of installation respectively, based on the method recommended by JGS (2002). Strain gauge readings were offset to be zero just before the start of the load test. During the load test, the load and displacement at the pile head were measured by a load cell and displacement transducers. The depth of the surface of the soil inside the pile (z_i) was measured at the center of the pile, using a steel bar and displacement transducers as shown in Figure 4.

The press-in conditions and load test conditions for Piles A and B are summarized in Tables 2, where l_d and l_u is the downward and upward displacement in one cycle of surging, v_d and v_u are the downward and upward velocity, and v_r is the peripheral velocity of the pile.

3 RESULTS OF FIELD TESTS

3.1 *RCP pile (pile A)*

Figure 5 shows Q' and T' during installation of Pile A. The manually-set limitation of the jacking force (Q'_{UL}) was maintained very low when the pile was penetrating through a soft layer, with Q' being mostly

Table 2. Test conditions.

		Pile A	Pile B
Installation method		RCP	SP
l_d	mm	Arbitrary (manual)	
l_u	mm	Arbitrary (manual)	
v_d	m/min	0.5-0.7	0.7-2.1
v_u	m/min	1.8	1.8-2.6
v_r	rpm	7-11	-
f_w	L/min	15	-
Curing period	day	57	25

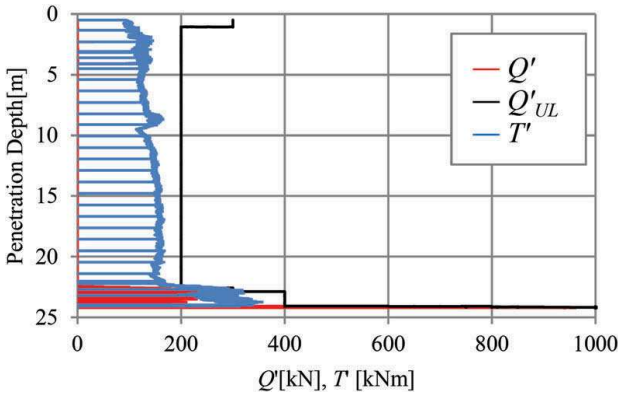

Figure 5. Jacking force and torque during installation.

zero (i.e. the pile was installed by a load smaller than the weight of the chucking part of the press-in machine), leading to little necessity of load-controlled surging. It then increased to greater values in the hard sand-gravel layer, leading to higher extent of load-controlled surging.

Figure 6 shows the variation of Q'_T with time at the end of installation. Q'_T was maintained at 950kN for about 15 minutes. The pile head displacement during this load test was measured to be 112mm, but this value is unreliable as it was measured by a sensor equipped in the press-in machine, which cannot remove the additional displacement associated with the

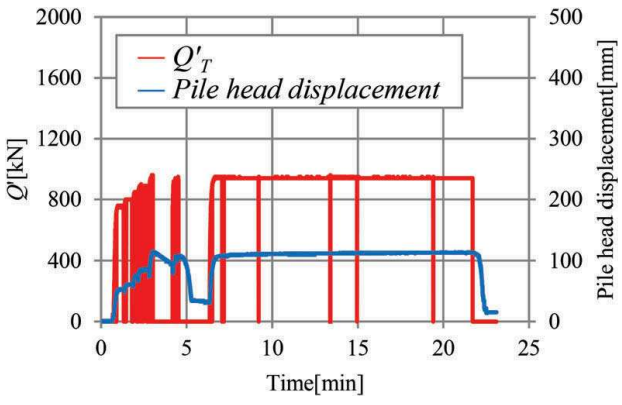

Figure 6. Axial force at the end of installation.

inclination of the press-in machine under a large jacking force.

Figure 7 shows the variation of the head load (Q) with time during the vertical static load test. As can be seen from this figure, the loading was conducted by multi-cycles and step sequence (with 5 cycles and 11 steps).

Figure 8 shows the variations of Q, base resistance (Q_b) and shaft resistance (Q_s) with the pile base displacement (δ_b) during the load test. Q_s showed its peak when δ_b reached around 10mm (= 1/100 D_o), and slightly decreased to its residual value until δ_b reached 80mm. Q_b continuously increased with the increasing δ_b. This continuous increase may partly be due to the small embedment length into the hard layer (bearing stratum). Defining the pile capacities as the values recorded when δ_b became 1/10 of D_o (JGS, 2002), the total capacity (Q_f), base capacity (Q_{bf}) and shaft capacity (Q_{sf}) were obtained as 5000kN, 3102kN and 1898kN, respectively. On the other hand, according to JGS (2002), the first-limit- resistance (Q_y, yielding load) can be obtained by plotting the relationship between head load and pile head displacement as shown in Figure 9 and by judging as the load giving the maximum curvature. As a result, Q_y of Pile A can be judged as 3000kN. The obtained values of Q_f, Q_{bf}, Q_{sf} and Q_y are summarized in Table 3.

Figure 10 shows the distribution of the axial load and the averaged unit shaft resistance (fs) with

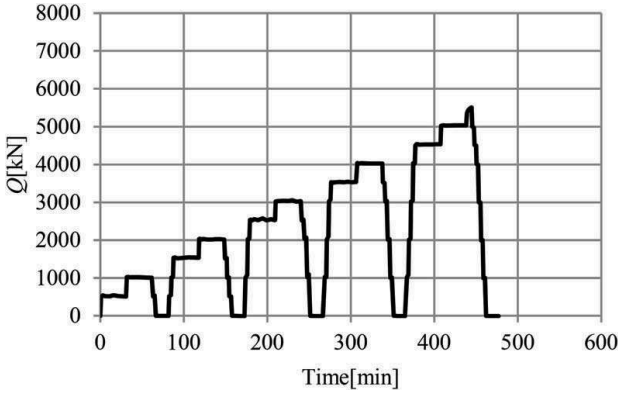

Figure 7. Loading record during load test.

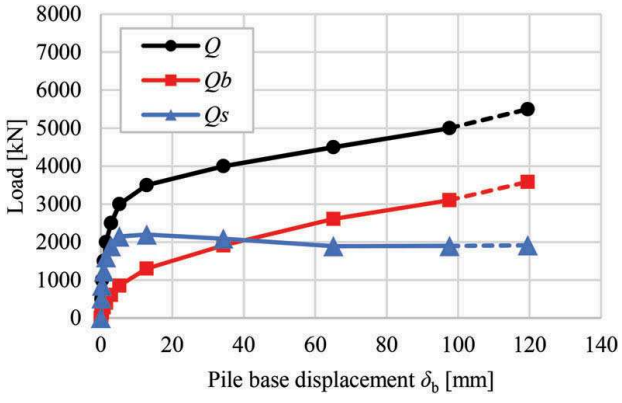

Figure 8. Load-Displacement relationship during load test.

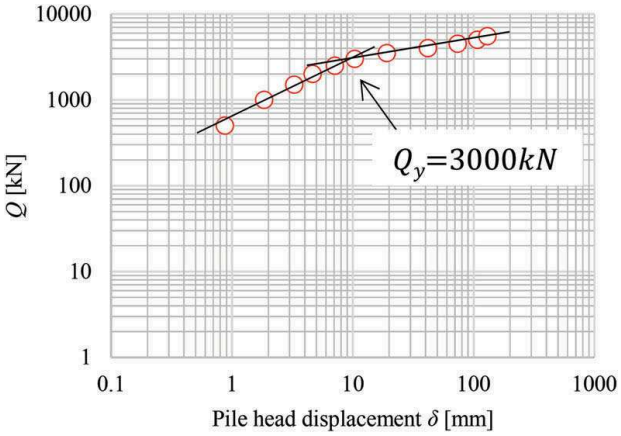

Figure 9. Determination of first-limit resistance.

Table 3. Result of load test on Pile A.

	kN
Q_f	5000
Q_{bf}	3102
Q_{sf}	1898
Q_y	3000

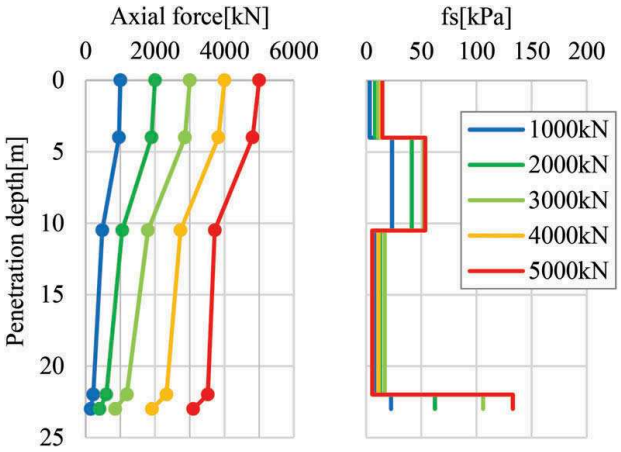

Figure 10. Distribution of axial force and fs.

depth, recorded at different load steps. It is clearly seen that the major part of the shaft resistance was generated in soil layers which contains sands or sand and gravels.

Figure 11 shows the increment of the inner soil column surface depth (z_i, as illustrated in Figure 12) plotted against the pile head displacement (δ) during the load test. It can be confirmed that the pile was fully plugged during the load test, if the plugging condition is defined by Incremental Filling Ratio (the ratio of the increment in z_i to the increment in δ). By the way, according to AIJ (2019), Q_{bf} of a closed-ended pile in the smallest case (for bored piles) is obtained by:

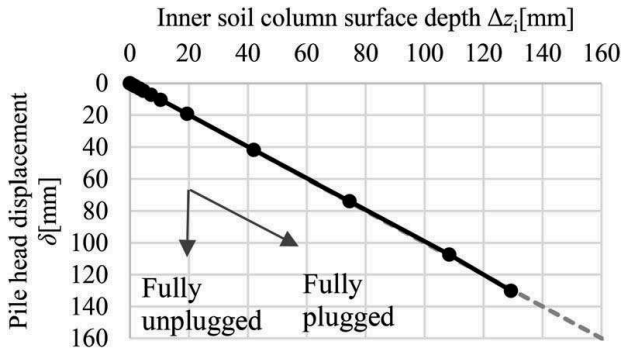

Figure 11. Inner soil column surface depth during loading test.

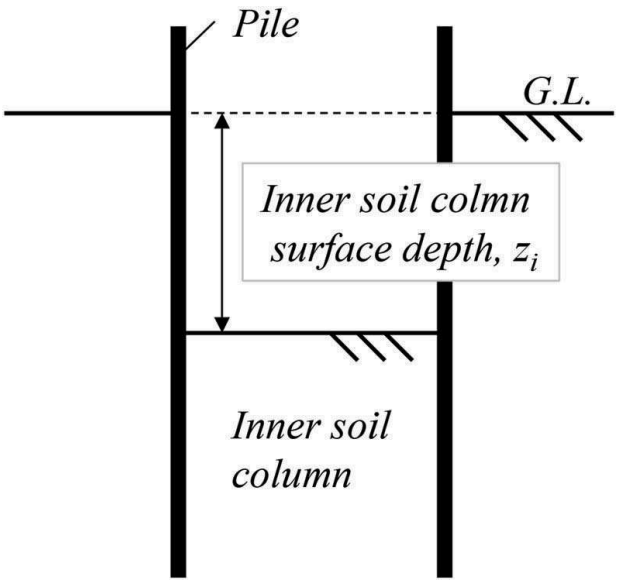

Figure 12. Definition of plugging.

$$Q_{bf} = min(150 \times N_D, 9000) \times A_{b,closed} \quad (1)$$

where $A_{b,closed}$ is the net cross-sectional area of a closed-ended pile. If the Pile A during the load test is assumed to be closed-ended based on the observation in Figure 11, Eq. (1) provides a significant overestimation (Q_{bf} = 7065kN). It is suggested that a compression of the inner soil is occurring during the load test.

3.2 *SP pile (Pile B)*

Figure 13 shows Q' during installation of Pile B. The pile was installed with surging manually. The manually-set limitation of the jacking force (Q'_{UL}) was maintained very low. It then increased to greater values in the sand layer, but a higher extent of load-controlled surging was exerted.

Figure 14 shows the variation of Q'_T with time at the end of installation. Q'_T was maintained at 650kN for about 8 minutes, and the pile head displacement during this maintained load was about 275mm,

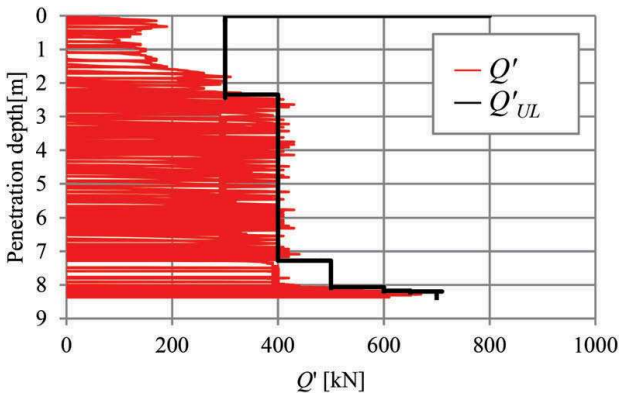

Figure 13. Jacking force during installation.

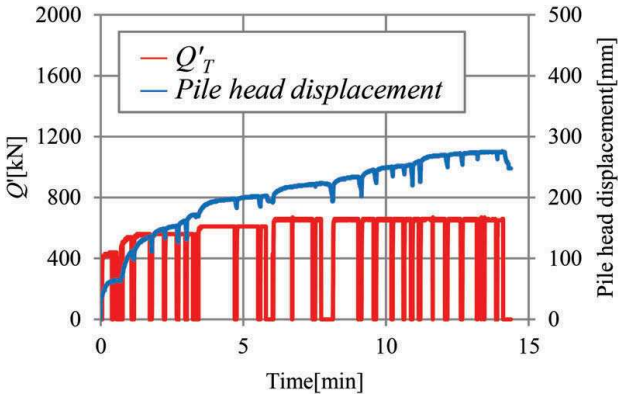

Figure 14. Axial loading at the end of installation.

which is unreliable due to the same reason as explained for Pile A.

Figure 15 shows the variation of the head load (Q) with time during the vertical static load test. As can be seen from this figure, the loading was conducted by multi-cycle step loading (with 6 cycles and 20 steps).

Figure 16 shows the variation of Q with the pile head displacement (δ) during the load test. Defining the total capacity (Q_f) as the load recorded when the pile head (not base, due to the lack of base displacement measurement) displacement reached 1-/10 of D_o, Q can be obtained as 1300kN.

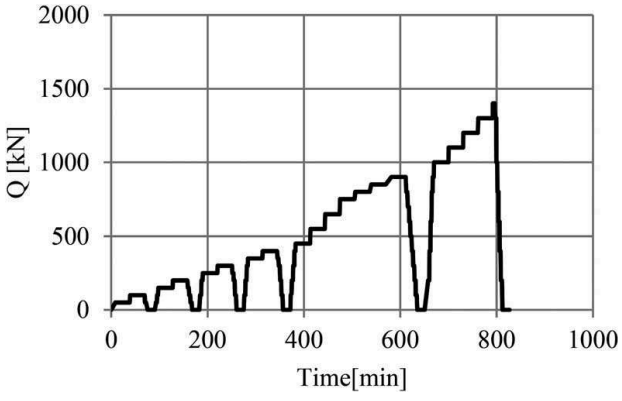

Figure 15. Loading record during load test.

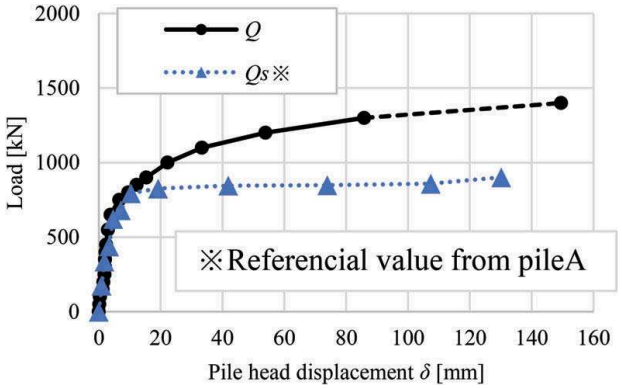

Figure 16. Load-Displacement relationship during load test.

The base and shaft resistances during the load test on Pile B are unknown, as this pile was not instrumented with axial strain gauges. Here, it is attempted that the shaft resistance (Q_s) on Pile B is roughly estimated based on the results on Pile A in Figure 10, ignoring the effect of differences in the piling method and the pile length. Figure 16 shows the variation of Q_s on Pile A in the depth range of 0m < z < 8m (corresponding to the embedment depth of Pile B), plotted against δ (not δ_b). It is seen that Q_s became constant at 860kN when δ is greater than 20mm. Adopting this Q_s value as the shaft capacity of Pile B, Q_b of Pile B can be estimated as 440kN. On the other hand, Figure 17 shows the relationship between the head load and the rate of pile head displacement recorded at different loading steps during the load test, by which Q_y can be judged as 1000kN (as the load giving the maximum curvature). The obtained values of Q_f, Q_{bf}, Q_{sf} and Q_y are summarized in Table 4.

Figure 18 shows the increment of the inner soil column surface depth (z_i, as illustrated in Figure 12) plotted against the pile head displacement (δ) during the load test. It can be confirmed that the plugging condition of Pile B shifted from a fully-plugged condition (for δ < 80mm) to a partially plugged condition (for δ > 80mm). This value of δ (≒ 80mm) corresponds to the point of time when the head load

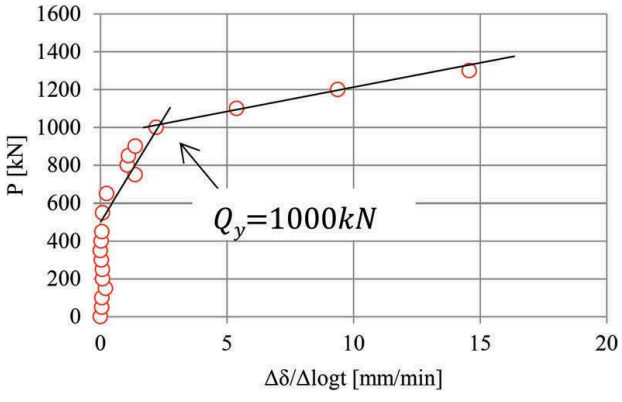

Figure 17. Determination of First-limit resistance

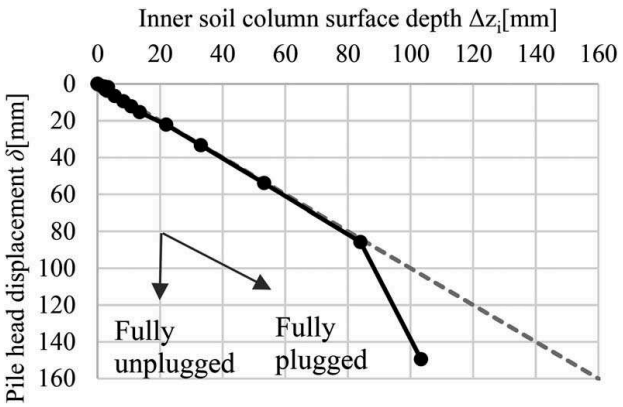

Figure 18. Inner soil column surface depth during loading test.

Table 4. Result of load test on Pile B.

	kN
Q_f	1300
Q_{bf}	440
Q_{sf}	860
Q_y	1000

became unmaintainable as expressed by a dotted line in Figure 16, but the shift of the plugging condition does not appear to be reflected in this load-displacement curve (i.e. the load appears to be increasing continuously).

4 CONCLUSIONS

The records of installation and the results of static vertical load tests on two piles with the outer diameter of 1000mm and the thickness of 12mm were reported.

Pile A had its embedment depth of 24m and was installed by Rotary Cutting Press-in into a bearing stratum consisting of a sand and gravel layer with SPT *N* value exceeding 50. It was instrumented with strain gauges at several sections for measuring axial strains. Axial jacking force of 950kN was applied at the end of installation without rotation. The load test was conducted 57 days after the end of installation. The obtained base and shaft capacities were approximately 3000kN and 2000kN respectively. The plugging condition, judged by *IFR* (Incremental Filling Ratio), was fully plugged during the load test.

Pile B had its embedment depth of 8m and was installed by Standard Press-in into a loose silty sand layer with SPT *N* value around 19. Axial jacking force of 600kN was applied at the end of installation. The load test was conducted 25 days after the end of installation. The obtained total capacity was around 1300kN. Shaft capacity was estimated to be 860kN, from the axial loads recorded in the corresponding

depth range in Pile A. The plugging condition shifted from fully plugged to partially plugged, but this transition did not apparently influence the load displacement curve.

REFERENCES

Architectural Institute of Japan (AIJ). 2019. Recommendations for Design of Building Foundations, 196p. (in Japanese)

International Press-in Association (IPA). 2016. *Press-in retaining structures: a handbook*, *First edition 2016*, 520p.

The Japanese Geotechnical Society (JGS). 2002. Method for static axial compressive load test of single piles. *Standards of Japanese Geotechnical Society for Vertical Load Tests of Piles*, pp. 49–53.

Tanaka, K., Kimizu, M., Otani, J. and Nakai, T. 2018. Evaluation of effectiveness of PFS Method using 3D finite element method. *Proceedings of the First International Conference on Press-in Engineering 2018, Kochi*, pp. 209–214.